On the properness condition for modal analysis of non symmetric second order systems

Morvan OUISSE

FEMTO-ST Institute - Department of Applied Mechanics - 24, rue de l'épitaphe - 25000 Besançon - FRANCE

Emmanuel FOLTÊTE

Abstract

Non symmetric second order systems can be found in several engineering contexts, including vibroacoustics, rotordynamics, or active control. In this paper, the notion of properness for complex modes is extended to the case of non self-adjoint problems. The properness condition is related to the ability of a set of complex modes to represent in an exact way the behavior of a physical second order system, meaning that the modes are the solutions of a quadratic eigenvalue problem whose matrices are those of a physical system. This property can be used to identify the damping matrices which may be difficult to obtain with mathematical modeling techniques. The first part of the paper demonstrates the properness condition for non symmetric systems in general. In the second part, the authors propose a methodology to enforce that condition in order to perform an optimal reconstruction of the "closest" physical system starting from a given basis complex modes. The last part is dedicated to numerical and experimental illustrations of the proposed methodology. A simulated academic test case is first used to investigate the numerical aspects of the method. A physical application is then considered in the context of rotordynamics. Finally, an experimental test case is presented using a structure with an active control feedback. An extension of the LSCF identification technique is also introduced to identify both left and right complex mode shapes from measured frequency response functions.

Keywords: properness condition, complex modes, non symmetric second order system, experimental modal analysis, damping identification

1. Introduction

Experimental modal analysis is a very commonly employed tool in structural dynamics. Indeed, given the identified modal parameters (eigenfrequencies, eigenvectors, modal damping ratios and modal masses), the dynamic response of a structure to an arbitrary excitation can be readily evaluated at the measured degrees of freedom. The experimentally identified eigensolutions can also be used to construct a reduced dynamic model which conserves some of the physical properties of the system, for example the system topology, mass, and stiffness characteristics. While the mass and stiffness properties can often be accurately represented with mathematical modeling techniques (e.g. finite element analysis), the mechanisms of energy dissipation remain notoriously difficult to simulated numerically and the present paper focuses on this particular point.

It has been shown [1] that for structural dynamics problems with symmetric matrices, the existence of an equivalent physical experimental reduced model is equivalent to the so-called properness condition of complex vectors. Moreover, in this same paper, an efficient methodology has been proposed to enforce that property when identified modes do not verify the properness condition.

Email addresses: morvan.ouisse@univ-fcomte.fr (Morvan OUISSE), emmanuel.foltete@univ-fcomte.fr (Emmanuel FOLTÊTE)

However, some structural dynamics applications lead to non symmetric second-order formulations, such as vibroacoustics problems [2] or rotordynamics problems [3]. For these systems, a quadratic eigenvalue problem [4] must be solved to obtain a coherent modal description of the problem, using left and right complex modes. In this paper, we propose to extend the symmetric properness condition to non symmetric systems. Section 2 provides a brief overview of the classical modal properties of non symmetric second-order problem. Section 3 proposes an extension of the properness condition to non self adjoint problems and the associated inverse relations for reconstructing the reduced system matrices from experimental data. These new relations are almost trivial to obtain but constitute important results for experimental matrix identification. Section 4 presents an original technique for optimally correcting the left and right eigenvectors in order to satisfy the properness condition. A non-classical Riccati equation is derived from a constrained minimization problem and a numerical procedure is proposed to solve it. The corrected eigenvectors can then be used for the optimal reconstruction of the reduced system matrices. Section 4 presents a non-physical numerical test-case to investigate the numerical aspects of the method. A physical application is then considered in section 5 in the context of rotordynamics. Finally, an experimental test-case is presented in section 6 using a structure with an active control feedback. An extension of the LSCF identification technique is also proposed to identify both left and right complex mode shapes from measured frequency response functions.

2. Problem description and modal decomposition

This section describes the typical problem which is considered in this paper and reviews the classical modal properties of non-self adjoint problems.

2.1. Second-order typical problem

The second-order problem which is considered in this paper is given by:

$$[M]\{\ddot{q}(t)\} + [C]\{\dot{q}(t)\} + [K]\{q(t)\} = \{f(t)\}, \tag{1}$$

where:

- $\{q(t)\}$ is the vector of the unknown discretized field,
- $[M]$ is the mass matrix, assumed to be nonsingular, that is to say, all eigenvalues of $[M]$ are finite,
- $[K]$ is the stiffness matrix,
- $[C]$ is the damping matrix,
- $\{f(t)\}$ is the force vector.

All system matrices are also assumed to be real, but not necessarily symmetric. The notations used here are in accordance with those proposed in [5]. In particular, brackets are used for matrices and curly braces are used for vectors.

These time-domain equations correspond to the following direct quadratic eigenvalue problem:

$$\left([M]\lambda_j^2 + [C]\lambda_j + [K]\right)\{\phi_{Rj}\} = 0, \tag{2}$$

and the associated adjoint eigenvalue problem:

$$\left([M]^T\lambda_j^2 + [C]^T\lambda_j + [K]^T\right)\{\phi_{Lj}\} = 0, \tag{3}$$

where λ_j is the j-th eigenvalue associated to the j-th right eigenvector $\{\phi_{Rj}\}$ and j-th left eigenvector $\{\phi_{Lj}\}$.

Since the matrices are not necessarily symmetric, the eigenvalues of the problem are real or come in pairs (λ_j, λ_j^*). If $\{\phi_j\}$ is a (right or left) eigenvector associated to λ_j, then $\{\phi_j^*\}$ is a (right or left) eigenvector associated to λ_j^*. A thorough review of this problem can be found in [4].

2.2. Modal decomposition of the permanent harmonic response

The eigenmodes of the system can be efficiently used in particular for the modal decomposition of the permanent harmonic response. This can be done considering the state-space representation of the system:

$$[U]\left\{\dot{Q}(t)\right\} - [A]\{Q(t)\} = \{F(t)\}, \tag{4}$$

in which:

$$\begin{array}{c} [U] = \begin{bmatrix} C & M \\ M & 0 \end{bmatrix},\ [A] = \begin{bmatrix} -K & 0 \\ 0 & M \end{bmatrix}, \\ \{Q(t)\} = \begin{Bmatrix} q(t) \\ \dot{q}(t) \end{Bmatrix},\ \{F(t)\} = \begin{Bmatrix} f(t) \\ 0 \end{Bmatrix}. \end{array} \tag{5}$$

The eigenvalues of this problem can be stored in the spectral matrix Λ:

$$[\Lambda] = \left[\backslash \lambda_j \backslash\right]. \tag{6}$$

The $j-th$ eigenvalue is associated to:

- a right eigenvector $\{\theta_{Rj}\}$ such as $(U\lambda_j - A)\{\theta_{Rj}\} = 0$, in which $\{\theta_{Rj}\} = \begin{Bmatrix} \phi_{Rj} \\ \phi_{Rj}\lambda_j \end{Bmatrix}$. Storing the eigenvectors (in the same order as the eigenvalues) in the modal matrix $[\theta_R] = \begin{bmatrix} \phi_R \\ \phi_R\Lambda \end{bmatrix}$, the following relationship is verified:
$$[U][\theta_R][\Lambda] = [A][\theta_R]. \tag{7}$$
- a left eigenvector $\{\theta_{Lj}\}$ such as $\{\theta_{Lj}\}^T(U\lambda_j - A) = 0$, in which $\{\theta_{Lj}\} = \begin{Bmatrix} \phi_{Lj} \\ \phi_{Lj}\lambda_j \end{Bmatrix}$. Storing the eigenvectors (in the same order as the eigenvalues) in the modal matrix $[\theta_L] = \begin{bmatrix} \phi_L \\ \phi_L\Lambda \end{bmatrix}$, the following relationships are verified:
$$[U]^T[\theta_L][\Lambda] = [A]^T[\theta_L] \quad \text{or} \quad [\Lambda][\theta_L]^T[U] = [\theta_L]^T[A]. \tag{8}$$

The orthogonality relationships can be written using $2n$ arbitrary values to construct the diagonal matrix $[\xi] = \left[\backslash \xi_j \backslash\right]$:

$$[\theta_L]^T[U][\theta_R] = [\xi] \ \text{ or } \ [\theta_L]^T[A][\theta_R] = [\xi][\Lambda]. \tag{9}$$

The modal decomposition of the permanent harmonic response at frequency ω is finally:

$$\{Q(t)\} = [\theta_R]\left([\xi]\left(j\omega[E_{2n}] - [\Lambda]\right)\right)^{-1}[\theta_L]^T\{F(\omega)\}e^{i\omega t}, \tag{10}$$

in which E_{2n} is the $2n \times 2n$ identity matrix and $F(\omega)$ is the complex amplitude of the harmonic excitation. This relationship can also be rewritten using the n degrees of freedom notation in the frequency domain:

$$\{q(\omega)\} = [\phi_R][\Xi][\phi_L]^T\{f(\omega)\}, \tag{11}$$

with:

$$[\Xi] = \left[\backslash \frac{1}{\xi_j(i\omega - \lambda_j)} \backslash\right]. \tag{12}$$

A classical way to use these modes is to evaluate the harmonic response based on the previous equations using a limited number of modes, depending on the maximum excitation frequency sought. In the field of experimental modal analysis, an experimental reduced model is built from complex modes which are identified from the FRFs (Frequency Response Functions) using techniques such as those described in [6, 7] for symmetric problems.

In the previous relationships, it should be emphasized that the size of the state-space modal matrices $[\theta_R]$ and $[\theta_L]$ is $2n \times 2n$, while the size of physical space modal matrices $[\phi_R]$ and $[\phi_L]$ is $n \times 2n$.

In what follows, it will be assumed, without loss of generality, that the eigenshapes are normalized such as $[\xi] = [E_{2n}]$.

3. Properness condition

The properness condition for the complex modes of symmetrical systems is described in detail in reference [1]. Starting from a given set of $2n$ identified complex modes, this condition is related to the fact that the system can be exactly represented in the frequency range of interest, by a n-degrees of freedom equivalent physical model, built from the identified modes. If a set of vectors does not verify the properness condition, this means that either the system can not be represented by this reduced set of modes, or that the experimental identification has introduced errors in the eigenshapes as the properness condition is very sensitive to noise. In this case, Balmès has proposed a methodology to enforce the properness condition in structural dynamics [1]. In the same paper, it is also shown that the properness condition is equivalent to the completeness of the basis, which is discussed for example in references [8] and [9]. In this section, the properness condition and associated matrix reconstruction relationships are extended to the case of non symmetric systems.

The properness condition is directly associated to the inverse problem defined by inverting the orthogonality conditions (9):

$$[U]^{-1} = [\theta_R]\,[\theta_L]^T \tag{13}$$

or

$$\begin{aligned}\begin{bmatrix} C & M \\ M & 0 \end{bmatrix}^{-1} &= \begin{bmatrix} 0 & M^{-1} \\ M^{-1} & -M^{-1}CM^{-1} \end{bmatrix} \\ &= \begin{bmatrix} \phi_R\phi_L^T & \phi_R\Lambda\phi_L^T \\ \phi_R\Lambda\phi_L^T & \phi_R\Lambda^2\phi_L^T \end{bmatrix},\end{aligned} \tag{14}$$

and

$$[A]^{-1} = [\theta_R]\,[\Lambda]\,[\theta_L]^T \tag{15}$$

or

$$\begin{aligned}\begin{bmatrix} -K & 0 \\ 0 & M \end{bmatrix}^{-1} &= \begin{bmatrix} -K^{-1} & 0 \\ 0 & M^{-1} \end{bmatrix} \\ &= \begin{bmatrix} \phi_R\Lambda^{-1}\phi_L^T & \phi_R\phi_L^T \\ \phi_R\phi_L^T & \phi_R\Lambda\phi_L^T \end{bmatrix}.\end{aligned} \tag{16}$$

It is then clear that the properness condition for non symmetric second order systems can be written as:

$$\left[\phi_R\phi_L^T\right] = 0. \tag{17}$$

Once this relationship is satisfied, the matrices can be found using the inverse relations:

$$M = \left[\phi_R\Lambda\phi_L^T\right]^{-1}, \tag{18}$$

$$K = -\left[\phi_R\Lambda^{-1}\phi_L^T\right]^{-1}, \tag{19}$$

$$C = -\left[M\phi_R\Lambda^2\phi_L^T M\right]. \tag{20}$$

In the context of symmetric systems, this is one of the most popular ways to identify damping matrices from experimental measurements. An important remark is that these relationships require the knowledge of n modes to build a n-degrees of freedom physical equivalent system. It should be emphasized that equations (17) to (20) are only valid if the normalization is such that $[\xi] = [E_{2n}]$, otherwise they could be written as:

$$\left[\phi_R\xi^{-1}\phi_L^T\right] = 0, \quad M = \left[\phi_R\xi^{-1}\Lambda\phi_L^T\right]^{-1}, \quad K = -\left[\phi_R\xi^{-1}\Lambda^{-1}\phi_L^T\right]^{-1}, \quad C = -\left[M\phi_R\xi^{-1}\Lambda^2\phi_L^T M\right]. \tag{21}$$

4. Enforcement of the properness condition

In this section, it is assumed that a modal identification has been performed and that the left and right eigensolutions have been identified from the measured FRFs. This step will be discussed in more detail when the experimental test case is presented. The objective is to perform an optimal correction of the eigenvectors in order to verify the properness condition (17). In practice, the identification of the experimental eigenshapes proves to be quite sensitive to measurement errors, and a small shift in the vectors can induce large changes not only in the properness relation but also in the values of reduced physical matrices after the inversion process. This will be illustrated later in the test-cases.
As such, the matrices $[\tilde{\phi}_R]$ and $[\tilde{\phi}_L]$ are sought that verify the properness relation (17) and that minimize the norm of $[\tilde{\phi}_R - \phi_R]$ and $[\tilde{\phi}_L - \phi_L]$. This problem can be written:

$$\begin{aligned} &\text{Find } [\tilde{\phi}_R] \text{ and } [\tilde{\phi}_L] \text{ minimizing } \left\|\tilde{\phi}_R - \phi_R\right\| \text{ and } \left\|\tilde{\phi}_L - \phi_L\right\| \\ &\text{with } [\tilde{\phi}_R \tilde{\phi}_L^T] = 0, \end{aligned} \tag{22}$$

in which $[\phi_R]$ and $[\phi_L]$ are two matrices of dimension $n \times 2n$ and $\|\cdot\|$ is a matrix norm.

A solution of this constrained minimization problem can be found using a Lagrange cost function H to be minimized with a Lagrange multiplier matrix $[\delta]$:

$$H = \frac{1}{2}\left\|\tilde{\phi}_R - \phi_R\right\| + \left\|\tilde{\phi}_L - \phi_L\right\| + [\delta] \otimes [\tilde{\phi}_R \tilde{\phi}_L^T], \tag{23}$$

where $\otimes$ represents a tensor product. The properness relation can be expanded based on the real and imaginary parts of the eigenshapes $[\tilde{\phi}_R] = [\tilde{\phi}_R^r] + i[\tilde{\phi}_R^i]$ and $[\tilde{\phi}_L] = [\tilde{\phi}_L^r] + i[\tilde{\phi}_L^i]$ giving:

$$[\tilde{\phi}_R \tilde{\phi}_L^T] = [\tilde{\phi}_R^r \tilde{\phi}_L^{rT}] - [\tilde{\phi}_R^i \tilde{\phi}_L^{iT}] + i[\tilde{\phi}_R^r \tilde{\phi}_L^{iT}] + i[\tilde{\phi}_R^i \tilde{\phi}_L^{rT}]. \tag{24}$$

Recalling that the complex eigenshapes are either real or come in pairs $\left(\{\phi_{Rj}\}, \{\phi_{Rj}^*\}\right)$ and $\left(\{\phi_{Lj}\}, \{\phi_{Lj}^*\}\right)$, it can be deduced that the imaginary part of the relation is always zero:

$$[\tilde{\phi}_R \tilde{\phi}_L^T] = Re\left([\tilde{\phi}_R \tilde{\phi}_L^T]\right) = [\tilde{\phi}_R^r \tilde{\phi}_L^{rT}] - [\tilde{\phi}_R^i \tilde{\phi}_L^{iT}]. \tag{25}$$

The Lagrange cost function to minimize can then be written using a real Lagrange multiplier matrix $[\delta]$:

$$H = \frac{1}{2}\left\|\tilde{\phi}_R - \phi_R\right\| + \left\|\tilde{\phi}_L - \phi_L\right\| + [\delta] \otimes Re\left([\tilde{\phi}_R \tilde{\phi}_L^T]\right). \tag{26}$$

A more explicit expression can be derived using the notations $[\tilde{\phi}] = [\phi] + [\Delta\phi]$ with $[\Delta\phi] = [\Delta\phi^r] + i[\Delta\phi^i]$ for the left and right eigenvectors:

$$\begin{aligned} H = \; & \frac{1}{2}\sum_{j,k}\left(\left(\Delta\phi_{Rjk}^r\right)^2 + \left(\Delta\phi_{Rjk}^i\right)^2 + \left(\Delta\phi_{Ljk}^r\right)^2 + \left(\Delta\phi_{Ljk}^i\right)^2\right) \\ & + \sum_{j,k,l}\delta_{jk}\left(\left(\phi_{Rjl}^r + \Delta\phi_{Rjl}^r\right)\left(\phi_{Lkl}^r + \Delta\phi_{Lkl}^r\right)\right. \\ & \qquad \left. - \left(\phi_{Rjl}^i + \Delta\phi_{Rjl}^i\right)\left(\phi_{Lkl}^i + \Delta\phi_{Lkl}^i\right)\right), \end{aligned} \tag{27}$$

where $\psi_{\alpha\beta}$ is the component (α, β) of matrix $[\psi]$. The minimization conditions for H leads to:

$$\frac{\partial H}{\partial \Delta\phi_{Rjk}^r} = 0 \Rightarrow \Delta\phi_{Rjk}^r + \sum_l \delta_{jl}\tilde{\phi}_{Llk}^r, \tag{28}$$

$$\frac{\partial H}{\partial \Delta\phi_{Ljk}^r} = 0 \Rightarrow \Delta\phi_{Ljk}^r + \sum_l \delta_{lj}\tilde{\phi}_{Rlk}^r, \tag{29}$$

$$\frac{\partial H}{\partial \Delta\phi^i_{Rjk}} = 0 \Rightarrow \Delta\phi^i_{Rjk} - \sum_l \delta_{jl}\tilde{\phi}^i_{Llk}, \tag{30}$$

$$\frac{\partial H}{\partial \Delta\phi^i_{Ljk}} = 0 \Rightarrow \Delta\phi^i_{Ljk} - \sum_l \delta_{lj}\tilde{\phi}^i_{Rlk}, \tag{31}$$

or, in a matrix form:

$$\begin{cases} [\Delta\phi^r_R] + [\delta\ \tilde{\phi}^r_L] = 0, \\ [\Delta\phi^r_L] + [\delta^T\tilde{\phi}^r_R] = 0, \\ [\Delta\phi^i_R] - [\delta\ \tilde{\phi}^i_L] = 0, \\ [\Delta\phi^i_L] - [\delta^T\tilde{\phi}^i_R] = 0. \end{cases} \tag{32}$$

Recombining the real and imaginary parts yields:

$$\begin{cases} [\tilde{\phi}_R] - [\phi_R] + [\delta\tilde{\phi}^*_L] = 0, \\ [\tilde{\phi}_L] - [\phi_L] + [\delta^T\tilde{\phi}^*_R] = 0. \end{cases} \tag{33}$$

Taking the complex conjugate of these two equations:

$$\begin{cases} [\tilde{\phi}^*_R] = [\phi^*_R] - [\delta\tilde{\phi}_L], \\ [\tilde{\phi}^*_L] = [\phi^*_L] - [\delta^T\tilde{\phi}_R], \end{cases} \tag{34}$$

and reinjecting the two previous equations gives:

$$\begin{cases} [\tilde{\phi}_R] - [\phi_R] + [\delta\phi^*_L] - [\delta\delta^T\tilde{\phi}_R] = 0, \\ [\tilde{\phi}_L] - [\phi_L] + [\delta^T\phi^*_R] - [\delta^T\delta\tilde{\phi}_L] = 0, \end{cases} \tag{35}$$

or:

$$\begin{cases} [\tilde{\phi}_R] = [E_n - \delta\delta^T]^{-1}[\phi_R - \delta\phi^*_L], \\ [\tilde{\phi}_L] = [E_n - \delta^T\delta]^{-1}[\phi_L - \delta^T\phi^*_R]. \end{cases} \tag{36}$$

The above equation provides an expression for the modified complex vectors when $[\delta]$ is known. To obtain the value of the Lagrange multipliers, the properness condition is written:

$$0 = [\tilde{\phi}_R\tilde{\phi}^T_L] = [E_n - \delta\delta^T]^{-1}[\phi_R - \delta\phi^*_L][\phi^T_L - \phi^{*T}_R\delta][E_n - \delta^T\delta]^{-T}. \tag{37}$$

This leads to a Riccati equation whose solution provides the value of the Lagrange multiplier matrix:

$$0 = [\phi_R\phi^T_L] - [\phi_R\phi^{*T}_R]\,[\delta] - [\delta]\,[\phi^*_L\phi^T_L] + [\delta]\,[\phi^*_L\phi^{*T}_R]\,[\delta]. \tag{38}$$

This equation is the generalization of the expression in reference [1]. It does not possess a unique solution. A necessary and sufficient condition for the solution to be a minimum of the cost function is that the matrix of the second order derivatives of H must be positive definite. In a matrix form, this can be written as:

$$\begin{bmatrix} E_n & \delta & 0 & 0 \\ \delta^T & E_n & 0 & 0 \\ 0 & 0 & E_n & -\delta \\ 0 & 0 & -\delta^T & E_n \end{bmatrix} > 0. \tag{39}$$

This symmetric matrix can be decomposed into four $2n \times 2n$ submatrices and it is definite positive if and only if the lower right block matrix and the Schur complement of the matrix are both definite positive:

$$\begin{bmatrix} E_n & \delta & 0 & 0 \\ \delta^T & E_n & 0 & 0 \\ 0 & 0 & E_n & -\delta \\ 0 & 0 & -\delta^T & E_n \end{bmatrix} > 0 \Leftrightarrow \begin{cases} \begin{bmatrix} E_n & \delta \\ \delta^T & E_n \end{bmatrix} > 0, \\ \begin{bmatrix} E_n & -\delta \\ -\delta^T & E_n \end{bmatrix} > 0. \end{cases} \tag{40}$$

The two $2n \times 2n$ matrices have the same Schur complement $[S]$, and they are definite positive if and only if $[S] = [E_n] - [\delta^T \delta] > 0$. This condition will be true if and only if the eigenvalues of $[\delta \delta^T]$ have a norm less than 1. Finding a solution of the Riccati equation that verifies this condition indicates that it is a minimum of the Lagrange cost function, even if it is not necessarily the global minimum.

The Riccati equation (38) is not identical to the one used in classical active control theory, since the matrices pre- and post-multiplying $[\delta]$ are not the transpose of one another. Nevertheless, an efficient method can be used to solve this equation using a Newton technique:

1. Start with $[\delta_0] = \epsilon [E_n]$ with $|\epsilon| << 1$.
2. Iterate: at step k, search for $[\Delta \delta_k]$ such as $[\delta_{k+1}] = [\delta_k] + [\Delta \delta_k]$ by solving the first-order polynomial matrix problem

$$[r_k] + [\, -\phi_R \phi_R^{*T} + \delta_k \phi_L^* \phi_R^{*T}\,]\,[\Delta \delta_k] + [\Delta \delta_k]\,[\, -\phi_L^* \phi_L^T + \phi_L^* \phi_R^{*T} \delta_k] = 0, \tag{41}$$

   with $[r_k] = [\phi_R \phi_L^T] - [\phi_R \phi_R^{*T}]\,[\delta_k] - [\delta_k \phi_L^* \phi_L^T] + [\delta_k]\,[\phi_L^* \phi_R^{*T}]\,[\delta_k]$.
3. Stop iterations when $\|r_k\|$ is less than a given threshold.

Equation (41) is a Sylvester equation that can be solved using several techniques among which the one proposed in reference [10]. It should be noted that the method proposed here to solve the Riccati equation may be inefficient in the context of active control, since in this case the "closest" solution to the initial value of $[\delta]$ which is found might not be the real-valued positive-definite solution corresponding to the steady-state optimal configuration of the control. However, in the present case, the optimal solution is assumed to be "close" to the initial state (i.e. the experimental identification is not too far from the "exact" solution), and the Newton algorithm is likely to converge to the solution of interest. Although there is no way to be sure that the stationary point is the global minimum of the cost function, the eigenvalue analysis of $[\delta \delta^T]$ will indicate that the point is a minimum or not.

5. Numerical illustration

A numerical illustration of the proposed methodology is presented in this section. A set of non-symmetric matrices are defined as starting point. These matrices do not correspond to any physical system and the purpose here is simply to illustrate the different steps in the identification process. In this example, the system matrices are taken to be:

$$[M] = \begin{bmatrix} 1.42 \times 10^{-2} & -2.44 \times 10^{-1} & -1.32 \times 10^{-1} & -3.43 \times 10^{-2} & -9.13 \times 10^{-2} \\ -5.30 \times 10^{-3} & 6.74 \times 10^{-1} & 6.00 \times 10^{-1} & 1.13 \times 10^{-1} & 3.72 \times 10^{-1} \\ -3.30 \times 10^{-3} & 2.20 \times 10^{-1} & 7.00 \times 10^{-4} & 6.90 \times 10^{-3} & 4.00 \times 10^{-2} \\ -6.00 \times 10^{-4} & 1.82 \times 10^{-1} & 9.87 \times 10^{-2} & 2.30 \times 10^{-2} & 7.22 \times 10^{-2} \\ -3.40 \times 10^{-3} & 5.13 \times 10^{-1} & 3.60 \times 10^{-1} & 7.27 \times 10^{-2} & 2.34 \times 10^{-1} \end{bmatrix}, \tag{42}$$

$$[C] = \begin{bmatrix} 2.23 \times 10^{0} & -1.09 \times 10^{1} & -1.63 \times 10^{1} & -3.90 \times 10^{0} & -8.95 \times 10^{0} \\ -7.62 \times 10^{0} & 1.52 \times 10^{1} & 3.31 \times 10^{1} & 9.61 \times 10^{0} & 1.88 \times 10^{1} \\ -2.05 \times 10^{0} & 2.24 \times 10^{1} & 2.58 \times 10^{1} & 5.59 \times 10^{0} & 1.478 \times 10^{1} \\ -1.82 \times 10^{0} & 1.00 \times 10^{1} & 1.42 \times 10^{1} & 3.37 \times 10^{0} & 7.97 \times 10^{0} \\ -5.38 \times 10^{0} & 1.88 \times 10^{1} & 3.13 \times 10^{1} & 8.16 \times 10^{0} & 1.76 \times 10^{1} \end{bmatrix}, \tag{43}$$

$$[K] = \begin{bmatrix} 1.33 \times 10^{2} & -1.06 \times 10^{2} & -2.10 \times 10^{2} & -9.30 \times 10^{1} & -1.35 \times 10^{2} \\ -1.28 \times 10^{2} & 7.02 \times 10^{1} & 3.61 \times 10^{2} & 1.36 \times 10^{2} & 2.20 \times 10^{2} \\ -2.31 \times 10^{2} & 1.63 \times 10^{2} & 4.32 \times 10^{2} & 1.78 \times 10^{2} & 2.63 \times 10^{2} \\ -1.04 \times 10^{2} & 7.42 \times 10^{1} & 2.20 \times 10^{2} & 8.98 \times 10^{1} & 1.36 \times 10^{2} \\ -1.84 \times 10^{2} & 1.26 \times 10^{2} & 3.85 \times 10^{2} & 1.57 \times 10^{2} & 2.37 \times 10^{2} \end{bmatrix}. \tag{44}$$

This system has 10 eigenvalues, which come in conjugate pairs. In the following expressions, the only eigenvalues (and associated eigenvectors) which are retained correspond to those with positive imaginary parts:

$$diag(\Lambda) = \begin{Bmatrix} -1.0943 \times 10^{1} + 4.5689\ i \times 10^{0} \\ -5.2119 \times 10^{-1} + 1.8209\ i \times 10^{1} \\ -2.1816 \times 10^{-1} + 2.9259\ i \times 10^{1} \\ -1.6913 \times 10^{0} + 3.5325\ i \times 10^{1} \\ -2.4968 \times 10^{0} + 4.8526\ i \times 10^{1} \end{Bmatrix}. \tag{45}$$

The real and imaginary parts of the associated right and left eigenvectors are:

$$Re\left([\phi_R]\right) = \begin{bmatrix} -3.26\times10^{1} & 3.13\times10^{1} & 1.84\times10^{1} & 6.92\times10^{1} & -4.58\times10^{1} \\ -4.83\times10^{1} & 3.09\times10^{1} & 3.12\times10^{1} & -2.80\times10^{1} & 2.77\times10^{1} \\ -4.57\times10^{1} & 2.17\times10^{1} & -4.21\times10^{1} & -6.19\times10^{2} & 9.79\times10^{2} \\ 1.18\times10^{0} & 6.01\times10^{1} & 2.56\times10^{0} & -3.84\times10^{1} & -6.93\times10^{1} \\ 2.82\times10^{2} & -5.02\times10^{1} & -6.20\times10^{1} & 4.13\times10^{1} & -3.45\times10^{1} \end{bmatrix}, \tag{46}$$

$$Im\left([\phi_R]\right) = \begin{bmatrix} 1.12\times10^{1} & -3.01\times10^{1} & -1.97\times10^{1} & -8.08\times10^{1} & -3.34\times10^{1} \\ 2.63\times10^{1} & -2.74\times10^{1} & -2.52\times10^{1} & 1.54\times10^{1} & 7.47\times10^{2} \\ 6.19\times10^{1} & -1.95\times10^{1} & 1.97\times10^{2} & 4.59\times10^{2} & 9.51\times10^{2} \\ 6.03\times10^{1} & -3.50\times10^{0} & -2.54\times10^{0} & 1.69\times10^{0} & -2.19\times10^{1} \\ -1.17\times10^{0} & 2.06\times10^{0} & 1.54\times10^{0} & -1.31\times10^{0} & -3.91\times10^{1} \end{bmatrix}, \tag{47}$$

$$Re\left([\phi_L]\right) = \begin{bmatrix} -3.34\times10^{1} & 3.11\times10^{1} & 1.81\times10^{1} & 6.726\times10^{1} & -4.47\times10^{1} \\ -1.89\times10^{1} & -1.03\times10^{0} & 4.83\times10^{2} & -2.92\times10^{1} & 4.19\times10^{1} \\ -4.86\times10^{1} & -7.73\times10^{1} & -2.68\times10^{3} & -1.24\times10^{1} & -2.31\times10^{1} \\ -4.15\times10^{1} & 1.24\times10^{0} & -8.91\times10^{1} & 6.52\times10^{1} & 1.63\times10^{0} \\ 6.62\times10^{1} & 9.48\times10^{1} & 7.70\times10^{1} & 6.10\times10^{1} & -1.11\times10^{0} \end{bmatrix}, \tag{48}$$

$$Im\left([\phi_L]\right) = \begin{bmatrix} 1.13\times10^{1} & -2.87\times10^{1} & -1.87\times10^{1} & -8.29\times10^{1} & -3.44\times10^{1} \\ -1.27\times10^{2} & 6.96\times10^{1} & -3.22\times10^{1} & 4.77\times10^{1} & 3.90\times10^{1} \\ 2.31\times10^{1} & 4.14\times10^{1} & -1.26\times10^{1} & 8.49\times10^{2} & -1.86\times10^{1} \\ 2.76\times10^{0} & 3.47\times10^{0} & -3.33\times10^{0} & -6.53\times10^{1} & 1.13\times10^{0} \\ -1.83\times10^{0} & -2.96\times10^{0} & 1.77\times10^{0} & -6.47\times10^{1} & -9.72\times10^{1} \end{bmatrix}. \tag{49}$$

It should be recalled that for each retained eigenvector associated to an eigenvalue, the complex conjugate is also an eigenvector, associated to the complex conjugate of the eigenvalue. In other words, the modal matrices used in the calculations are $[\phi_R] = [Re\left([\phi_R]\right) + i\Im\left([\phi_R]\right) \quad Re\left([\phi_R]\right) - i\Im\left([\phi_R]\right)]$ and $[\phi_L] = [Re\left([\phi_L]\right) + i\ Im\left([\phi_L]\right) \ \Re\left([\phi_L]\right) - i\ Im\left([\phi_L]\right)]$.

The eigenvectors are then modified using a random noise of 10% on the relative amplitudes of both the real and imaginary parts, while the eigenvalues are modified in the same way with a 3% random noise. The difference in these noise levels reflects the fact that the experimental identification of the eigenvectors is always less precise than that of the eigenvalues.

A direct identification of the matrices using formulas (18) to (20) from the simulated experimental data leads to erroneous matrices (they are given in Appendix A.1).

The direct "visual" comparison between reference and identified matrices is not very informative, a matrix norm can be used to evaluate the reconstruction error between the reference matrix $[A_{ref}]$ and the identified matrix $[A_{id}]$:

$$\varepsilon(A_{id}, A_{ref}) = \frac{\|A_{id} - A_{ref}\|_F}{\|A_{ref}\|_F}, \tag{50}$$

where $\|A\|_F$ is the Frobenius norm of A. Using this indicator, the error norms for the mass, damping and stiffness matrices are:

$$\begin{cases} \varepsilon([M_{dir}], [M]) = 0.5116, \\ \varepsilon([C_{dir}], [C]) = 0.5426, \\ \varepsilon([K_{dir}], [K]) = 5.006. \end{cases} \tag{51}$$

These can be combined in a single error indicator:

$$\varepsilon_{tot} = \varepsilon([M_{dir}], [M]) + \varepsilon([C_{dir}], [C]) + \varepsilon([K_{dir}], [K]) = 6.060. \tag{52}$$

The reconstruction is clearly not very accurate and this is due to the fact that the properness condition is not verified by the noisy data. Indeed, while the reference eigenvectors have a properness norm which is about 4.5×10^{-12}, corresponding to a numerical threshold in the eigenvalue solver), the properness norm of the noisy eigenvectors is:

$$\left\|\phi_{Rdist}\phi_{Ldist}^T\right\|_F = 2.019. \tag{53}$$

The optimal correction of the eigenvectors in order to enforce the properness condition is then applied. Figure 1 shows the evolution of the norm of the properness matrix corresponding to the solution of Riccati equation at a given iteration of algorithm as described in section 4. The convergence rate is seen to be very fast and only a few iterations are required to reach the solution. The eigenvalues of $[\delta\delta^T]$ are:

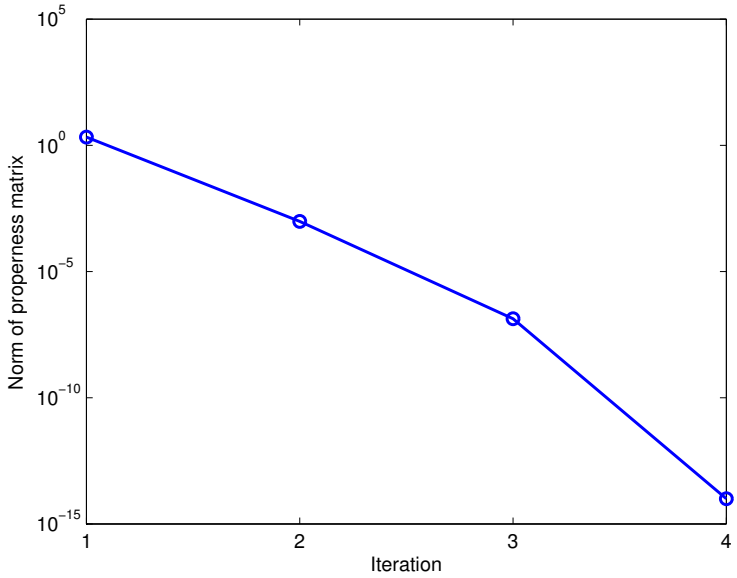

Figure 1: Convergence of the algorithm - Frobenius norm of the properness matrix versus iteration number

$$eig([\delta\delta^T]) = \left\{ \begin{array}{c} 6.8197 \times 10^{-6} \\ 8.2112 \times 10^{-6} \\ 5.1906 \times 10^{-5} \\ 1.4498 \times 10^{-4} \\ 7.9255 \times 10^{-3} \end{array} \right\}. \tag{54}$$

A stationary point of the Lagrange cost function has indeed been attained since each of the eigenvalues is less than one. Using this Lagrange multiplier matrix to modify the left and right eigenvectors leads to the corrected complex vectors that now verify the properness condition. Introducing these modes in the inverse relations gives the matrices shown in Appendix A.2.

Figure 2 shows the evolution of the relative error on the reconstructed matrices with the number of iterations. Even after the algorithm has converged, the errors between the original and reconstructed matrices are not zero since the reconstruction is based on noisy eigenvectors and the algorithm is searching for the "closest" system that has the same behavior. This closest system could be different from the original one, in particular when the noise levels are large. It is interesting to note that the matrix error index converges faster than the Lagrange multiplier matrix $[\delta]$. The final compact form for the matrices reconstruction error is:

$$\varepsilon_{tot} = 0.4290. \tag{55}$$

This simple simulated example suggests that the use of non proper eigenvectors has the greatest impact on the damping matrix. This observation is seen to be true in the following illustrations as well. It can be concluded that the identification of the damping matrix will no doubt fail if the properness condition is not enforced. In this sense, the proposed properness enforcement methodology can be understood as a physical regularization procedure.

The efficiency of the methodology can also be illustrated using FRFs. Figure 3 shows the following curves:

- The *Reference* FRF, calculated from the initial system matrices. For the purposes of illustration, only the collocated input-output FRF on the first degree of freedom is plotted here.

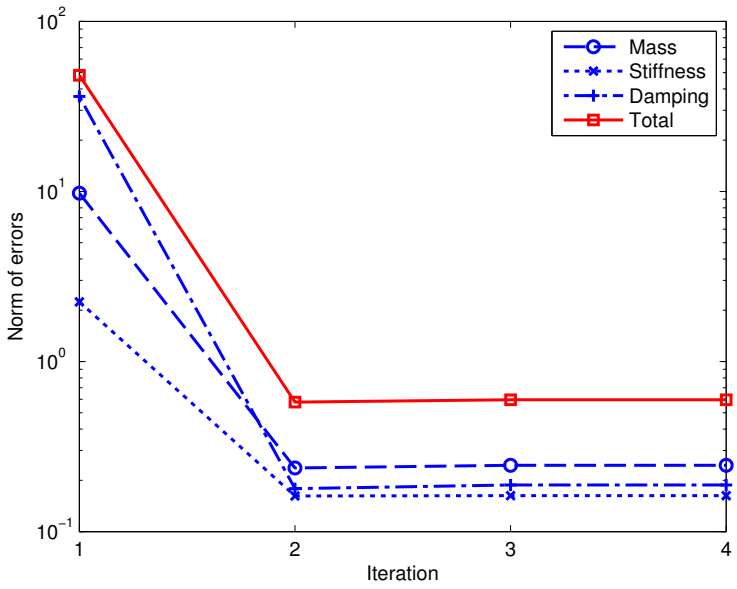

Figure 2: Evolution of errors on matrices versus iteration number in Newton algorithm

- The *Modal* FRF synthesized after the introduction of noise in the eigenvectors and simulating the experimentally identified eigensolutions. It is noted that this curve is visually coincident to the reference curve. In an experimental procedure, this would tend to indicate that the identification is correct. The relative error between the two curves is shown in figure 4 and will be discussed later.

- The *Direct* FRF reconstructed using the matrices obtained after solving the inverse problem from the eigenvalues and eigenvectors affected by noise. This procedure clearly fails in this case, because the properness condition is not strictly satisfied. It is seen here that even small differences in the experimental eigenproperties can induce large discrepancies in the identified system.

- The *Proper* FRF obtained using data with enforcement of the properness condition, to be discussed in the next paragraph. This curve is also visually coincident with the reference one.

It is important to note that when the properness condition is not satisfied, there is no equivalent system that is able to represent the behavior of the system with 5 degrees of freedom, and this is the reason why the direct reconstruction fails.

Figure 4 finally exhibits the relative errors of FRFs amplitudes for the disturbed configuration and both reconstructions. One can observe first that including some noise in the eigenvectors does not affect much the FRFs, which once again indicates that even with good values of criteria based on FRFs errors, the matrix reconstruction can be poor. The second observation concerns the enforcement of the properness condition that leads to errors which are very low compared to those obtained by direct reconstruction. One interesting trend is that the lowest values of error are obtained for frequencies corresponding to resonances of the system, while the maximum values are related to anti-resonances.

6. Rotordynamics application

A wide class of non self-adjoint problems can be found in rotordynamics applications. A whirling beam example, which has been described in [11], is considered here to illustrate the application of the method in this context. This high speed gyroscopic system includes a lumped mass at the center of the beam. The

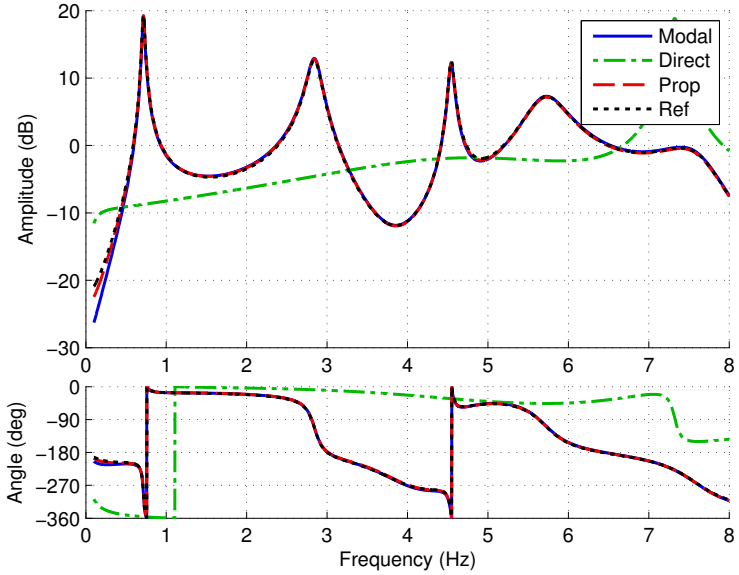

Figure 3: Comparison of FRFs - Original system (Ref), modal response of perturbed system (Modal), direct reconstruction (Direct), properness enforced reconstruction (Prop)

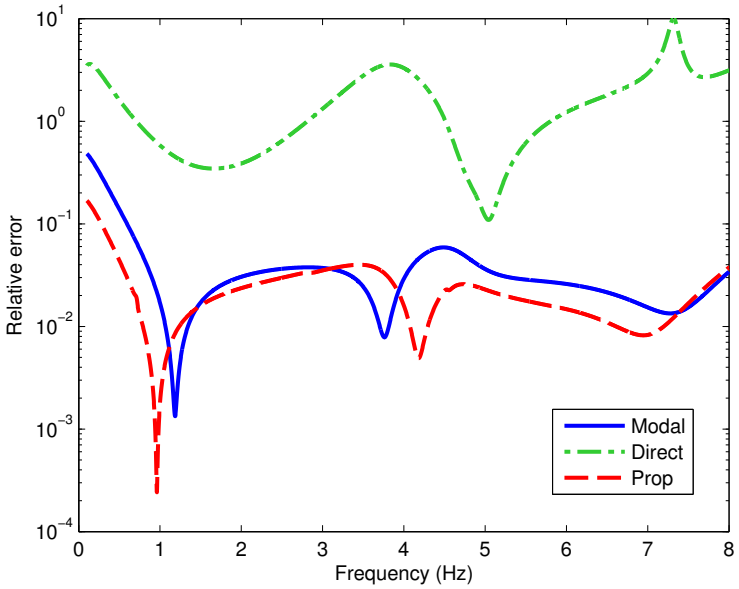

Figure 4: Comparison of relative errors in FRFs - Modal response on perturbed vectors, direct reconstruction, properness enforced reconstruction

system is discretized using 10 degrees of freedom, and the corresponding matrices (including gyroscopic and circulatory terms) are:

$$[M] = \begin{bmatrix} \mathcal{M} & 0 \\ 0 & \mathcal{M} \end{bmatrix}, \; [C] = \begin{bmatrix} \mathcal{C} & \mathcal{G} \\ -\mathcal{G} & \mathcal{C} \end{bmatrix}, \; [K] = \begin{bmatrix} \mathcal{K}^a & \mathcal{H} \\ -\mathcal{H} & \mathcal{K}^b \end{bmatrix}, \tag{56}$$

with the 5×5 defined by:

$$\begin{array}{l} \mathcal{M}_{pq} = mL\delta_{pq} + 2M\sin(p\pi/2)\sin(q\pi/2), \\ \mathcal{C}_{pq} = (c+h)L\delta_{pq}, \\ \mathcal{G}_{pq} = -2\Omega\mathcal{M}_{pq}, \\ \mathcal{K}^a_{pq} = 2\left(k_1 + (-1)^{p+q}k_2\right)pq\pi^2/L^2 + EI_x p^2q^2\pi^4/L^3\delta_{pq} - \Omega^2\mathcal{M}_{pq}, \\ \mathcal{K}^b_{pq} = 2\left(k_1 + (-1)^{p+q}k_2\right)pq\pi^2/L^2 + EI_y p^2q^2\pi^4/L^3\delta_{pq} - \Omega^2\mathcal{M}_{pq}, \\ \mathcal{H}_{pq} = -h\Omega L\delta_{pq}, \end{array} \tag{57}$$

where δ_{pq} is the Kronecker symbol, and the system properties are $m = 10$ kg.m^{-1}, $M = 10$ kg, $L = 5$ m, $EI_y = 9L^3/5\pi^2$ N.m^2, $EI_x = 4L^3/5\pi^2$ N.m^2, $k_1 = k_2 = L^2/20$ N.m, $\Omega = \sqrt{21.6}\pi$ rad.s^{-1}, $c = h = 0.25$ N.S.m^{-1}.

The complex eigenvalues and left and right eigenvectors are evaluated using the state-space form and random noise is added to the calculated real and imaginary values with a relative magnitude of 1% for eigenvalues and 3% for eigenvectors.

The system matrices are reconstructed both directly and with properness enforcement and the FRFs are evaluated from the reconstructed matrices. It is seen in figure 5 that the properness enforcement allows a correct synthesis of the FRFs, while the direct inverse technique leads to significant errors. The figure 6

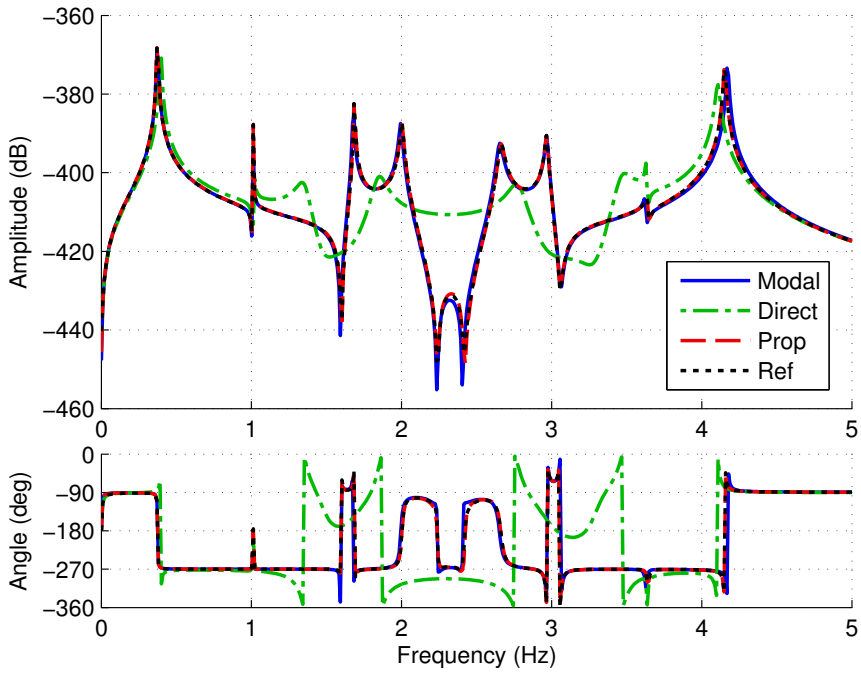

Figure 5: Frequency Response Functions between dofs 5 and 7 - Original system (Ref), modal response of disturbed system (Modal), direct reconstruction (Direct), properness enforced reconstruction (Prop)

shows the efficiency of the properness enforcement using a graphical representation of the system matrices, since the direct reconstruction introduces extra terms in matrices that lead to large errors in FRFs.

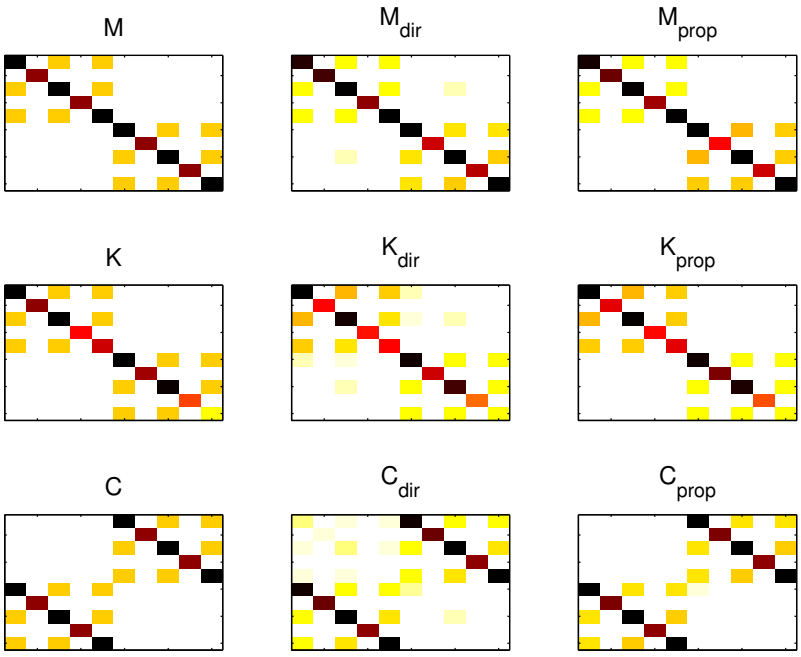

Figure 6: Graphical representation of matrices - Original system, direct reconstruction and reconstruction with properness enforcement (white = zero value, black = maximum amplitude)

7. Experimental illustration

7.1. Description of the experimental set-up

An experimental illustration of the proposed methodology is presented in this section. Figure 7 shows the experimental set-up comprising two beams which are coupled through their bases by a common clamping device. The frequency range of interest includes the first two modes of the coupled system which could be represented by an equivalent 2-degrees of freedom model, using points 1 and 2 indicated in figure 7 as reference points. These points are instrumented with accelerometers and contactless force transducers are used to excite the structure. An electrical intensity probe has also been used to check the value of the force sensors and to verify that the moving masses do not perturb the measured information. The system itself is characterized by symmetric matrices while the non symmetric parts are introduced using an active device.

The active part includes an Analogic Signal Processing (ASP) circuit, which introduces a force at point 3 depending on the value of displacement or acceleration at point 4. The results which are presented here correspond to a force feedback which is directly proportional to the displacement and is seen to be a non-symmetric term in the stiffness matrix. The gain of the feedback loop was chosen such that the system remains in the stable domain. All measurements have been performed using a sine-stepping approach to avoid undesirable effects due to broadband signal in the feedback loop.

7.2. Identification of the left and right modes

The classical LSCF method [7] can be easily adapted to identify the left and right complex modes of the structure. As indicated in [12], the full identification of the left and right vectors requires the use of sensors and excitations at every point of interest, that is to say, at every model degree of freedom. It should be noted that once the relationships between the left and right eigenvectors are available, this condition is no longer necessary and only a limited number of excitation points can be used. In the present case, no explicit relation exists between the left and right vectors and there is thus no alternative to exciting the structure at all points of interest. As such, an extension of the LSCF technique for non-self adjoint problem has to be considered.

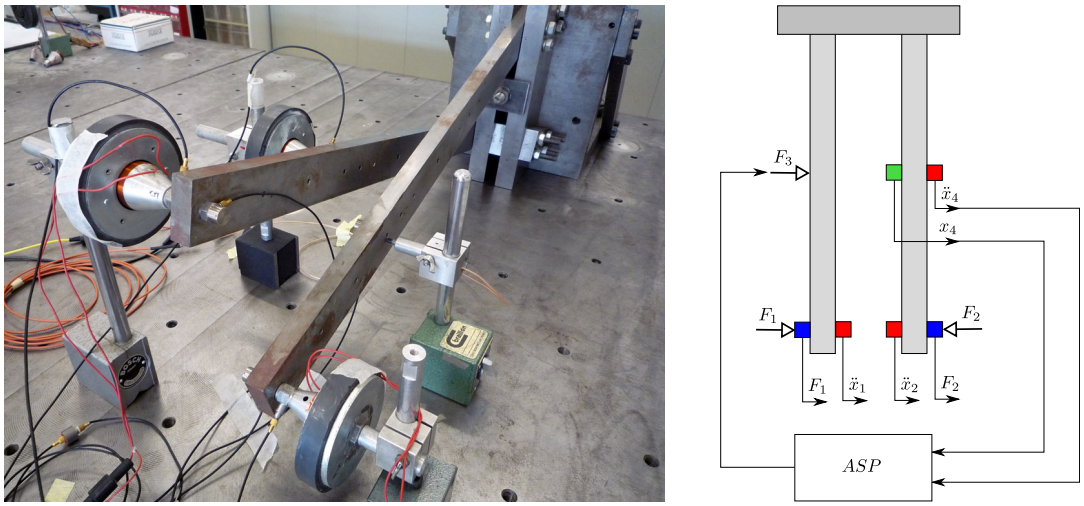

Figure 7: Experimental set-up with analogical loop

The identification procedure is based on the complex curve-fitting of the FRF matrix $[H(\omega)]$ which can be written using equation (11) with $\xi_j = 1$:

$$[H(\omega)] = \sum_{j=1}^{2n} \frac{\{\phi_{Rj}\}\{\phi_{Lj}\}^T}{i\omega - \lambda_j}. \tag{58}$$

The first step of the method is to identify the complex poles λ_j, and this can be done in exactly the same way as if the system were symmetric, since the eigenvalue is common to the left and right eigenvectors. Once the poles have been identified, the eigenvectors can be extracted.

The excitation of degree of freedom number j allows the residue matrix to be identified:

$$[R_j] = [\phi_R]\,[L_j], \tag{59}$$

where $[L_j]$ can be seen as the modal participation matrix which is diagonal and whose terms are the unknown j-th components of each left vector. This indicates that each column of $[R_j]$ is proportional to a right eigenvector. Since this matrix can be evaluated for each excitation point, an efficient way to find the orientation of right eigenvectors is to normalize the columns of $[R_j]$ to obtain a modified matrix $[\hat{R}_j]$, and to use the mean of all measured values to construct the direction of the right eigenvectors:

$$[\hat{\phi}_R] = \frac{1}{n}\sum_{j=1}^{n}[\hat{R}_j]. \tag{60}$$

The matrix $[\hat{\phi}_R]$ includes right eigenvectors such as $\xi_j = 1$ which are not yet normalized and this point will be discussed later. During the normalization operation which is performed on $[R_j]$, care must be taken with respect to the direction of the vectors to avoid opposite terms in equation (60), in particular if normalization of unit Euclidean norm is chosen.

The left eigenvectors can be found using an equivalent procedure based on dual residue matrices $[Q_j]$ which are composed of the rows j of all residue matrices $[R_j]$:

$$[Q_j] = \begin{bmatrix} R_1(j,:) \\ R_2(j,:) \\ \dots \\ R_n(j,:) \end{bmatrix}, \tag{61}$$

where $R(j,:)$ is the row j of matrix R. This matrix is the equivalent of R_j for the left eigenvectors. Its columns are then normalized to obtain $[\hat{Q}_j]$ and the left eigenvectors are then proportional to:

$$[\hat{\phi}_L] = \frac{1}{n}\sum_{j=1}^{n}[\hat{Q}_j]. \tag{62}$$

The final step is to change the norm of vectors in order that $\xi_j = 1$, which can be done by determining coefficients such that

$$[\phi_R] = [\hat{\phi}_R]\left[\backslash\alpha_{j\backslash}\right] \text{ and } [\phi_L] = [\hat{\phi}_L]\left[\backslash\alpha_{j\backslash}\right]. \tag{63}$$

The values of α_j can be evaluated using the diagonal terms of the residue matrices:

$$\alpha_j^2 = \frac{[R_j]_{jj}}{(\phi_{Lj})_j\,(\phi_{Rj})_j}, \tag{64}$$

or any other technique, such as least square minimization on all measured values. In the present case, the choice of the technique to evaluate α_j has a very small impact on the results since the key point is clearly the properness enforcement.

7.3. Results and discussion

The figure 8 shows two FRFs measured with an open loop excitation. The measured curve corresponds to the dotted line and the LSCF technique yields the complex modes and the corresponding modal synthesis (solid line). The modes are then used to identify the matrices using equations (18-20). Calculating the FRFs from these matrices leads to the dashdot line, while the dashed one corresponds to the synthetized FRFs obtained from complex vectors after properness enforcement. In this case the system should be symmetric,

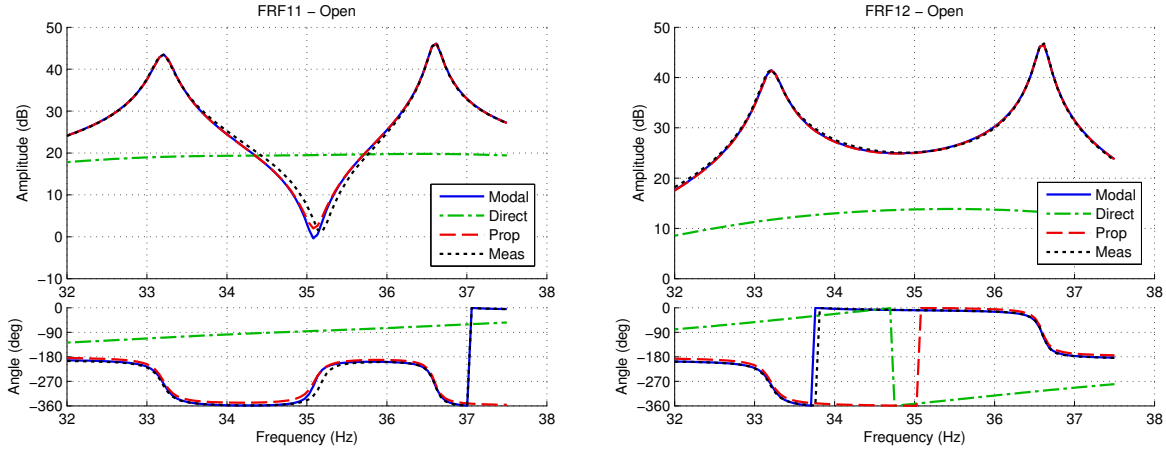

Figure 8: Examples of FRFs for open loop - Original system (Ref), modal synthesis from identified modes (Modal), direct reconstruction (Direct), properness enforced reconstruction (Prop)

and the direct reconstruction of the matrices fails because of the perturbation due to experimental noise.

The right and left eigenvectors which have been identified from the experimental FRFs are (the modal matrices are presented here without the complex conjugate terms):

$$\begin{aligned}[\phi_R^{open}] &= \begin{bmatrix} 0.0321 - 0.0373i & 0.0281 - 0.0326i \\ 0.0260 - 0.0301i & -0.0300 + 0.0351i \end{bmatrix}, \\ [\phi_L^{open}] &= \begin{bmatrix} 0.0327 - 0.0380i & 0.0284 - 0.0331i \\ 0.0237 - 0.0305i & -0.0296 + 0.0348i \end{bmatrix}. \end{aligned} \tag{65}$$

The properness enforcement leads to small changes in these vectors:

$$\begin{aligned}[\tilde{\phi}_R^{open}] &= \begin{bmatrix} 0.0350 - 0.0344i & 0.0301 - 0.0307i \\ 0.0283 - 0.0277i & -0.0328 + 0.0323i \end{bmatrix}, \\ \left[\tilde{\phi}_L^{open}\right] &= \begin{bmatrix} 0.0353 - 0.0355i & 0.0307 - 0.0307i \\ 0.0266 - 0.0277i & -0.0322 + 0.0323i \end{bmatrix}. \end{aligned} \tag{66}$$

The small modifications in complex vectors correspond to very large changes in the damping matrix. The matrices which are deduced from the original vectors are:

$$\begin{aligned}[M^{open}] = \begin{bmatrix} 0.536 & 0.0388 \\ 0.0308 & 0.632 \end{bmatrix}, \quad [C^{open}] = \begin{bmatrix} -17.0 & -2.84 \\ 0.296 & -23.7 \end{bmatrix}, \\ [K^{open}] = \begin{bmatrix} 2.53 \times 10^4 & -760 \\ -1.25 \times 10^3 & 3.07 \times 10^4 \end{bmatrix}, \end{aligned} \tag{67}$$

while those obtained after properness enforcement are:

$$\begin{aligned}[\tilde{M}^{open}] = \begin{bmatrix} 0.533 & 0.0377 \\ 0.0308 & 0.627 \end{bmatrix}, \quad [\tilde{C}^{open}] = \begin{bmatrix} 0.566 & 0.314 \\ 0.0688 & 0.848 \end{bmatrix}, \\ \left[\tilde{K}^{open}\right] = \begin{bmatrix} 2.52 \times 10^4 & -808 \\ -1.24 \times 10^3 & 3.05 \times 10^4 \end{bmatrix}. \end{aligned} \tag{68}$$

Once again, it can clearly be observed that the mass and stiffness matrices are relatively insensitive to the changes in the complex vectors, while the damping values are very affected by the properness enforcement. The corrected vectors clearly lead to a more physical damping matrix than the original ones and this corresponds to the behavior observed in figure 8.

These tests have been performed using the open loop circuit, which means that the system matrices should be symmetric. They are clearly not symmetric, but unlike those obtained from the original vectors, the extradiagonal terms of the matrices have the same signs and same order of magnitude. In the same way, the left and right complex vectors should be identical, which is not the case even if the differences are quite small. A better procedure would be to apply the methodology dedicated to symmetric systems which has been presented in [1]. The direct use of the methodology including symmetry constraints gives the following values for the mode shapes and matrices:

$$[\phi_R^{open}] = [\phi_L^{open}] = \begin{bmatrix} 0.0324 - 0.0377i & 0.0283 - 0.0328i \\ 0.0249 - 0.0303i & -0.0298 + 0.035i \end{bmatrix}, \tag{69}$$

$$\begin{aligned}[M^{open}] = \begin{bmatrix} 0.536 & 0.0348 \\ 0.0348 & 0.632 \end{bmatrix}, \quad [C^{open}] = \begin{bmatrix} -17.0 & -1.29 \\ -1.29 & -23.7 \end{bmatrix}, \\ [K^{open}] = \begin{bmatrix} 2.53 \times 10^4 & -1.00 \times 10^3 \\ -1.00 \times 10^3 & 3.07 \times 10^4 \end{bmatrix}, \end{aligned} \tag{70}$$

$$[\tilde{\phi}_R^{open}] = [\tilde{\phi}_L^{open}] = \begin{bmatrix} 0.0352 - 0.0349i & 0.0304 - 0.0307i \\ 0.0275 - 0.0277i & -0.0325 + 0.0323i \end{bmatrix}, \tag{71}$$

$$\begin{aligned}[\tilde{M}^{open}] = \begin{bmatrix} 0.533 & 0.0343 \\ 0.0343 & 0.627 \end{bmatrix}, \quad [\tilde{C}^{open}] = \begin{bmatrix} 0.569 & 0.194 \\ 0.194 & 0.848 \end{bmatrix}, \\ \left[\tilde{K}^{open}\right] = \begin{bmatrix} 2.52 \times 10^4 & -1.02 \times 10^3 \\ -1.02 \times 10^3 & 3.05 \times 10^4 \end{bmatrix}. \end{aligned} \tag{72}$$

All terms are in accordance with those obtained without the symmetry constraint. The differences correspond to uncertainties associated to experimental conditions.

A similar analysis can be performed with the closed loop excitation. In this case the system is not symmetric. The results presented here correspond to a gain value of 6 in the feedback loop, corresponding to a strong feedback that remains in the stable domain. Figure 9 shows two measured FRFs and the

corresponding synthesized ones using the identified complex modes, the matrices obtained by direct inversion and those corresponding to properness enforcement. It is clear once again that the properness enforcement yields very good results compared to the direct procedure.

Another point which can be observed is the impact of the feedback loop which induces shifts of the resonance peaks in comparison to the open loop (fig. 8). The modified LSCF technique presented in section

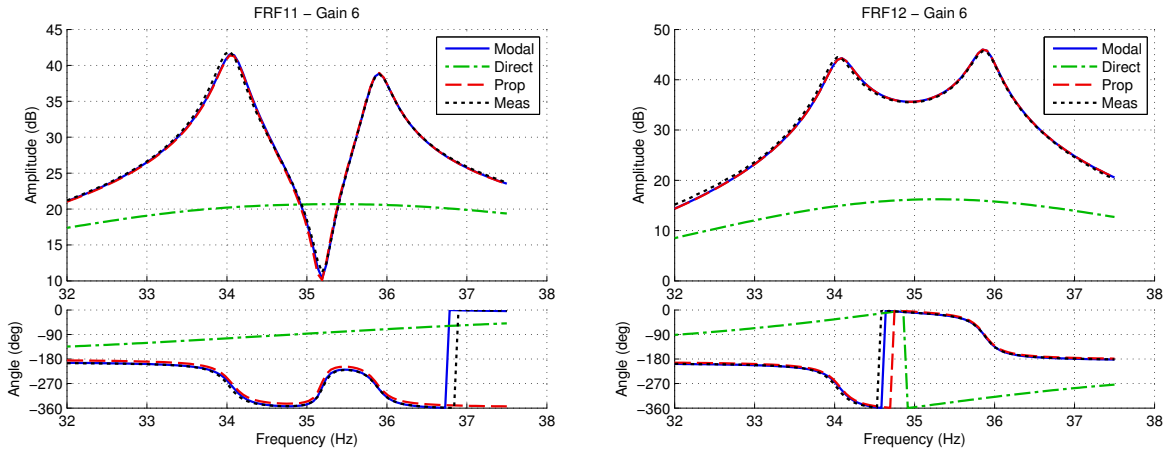

Figure 9: Examples of FRFs for closed loop with gain in 6th position - Original system (Ref), modal synthesis from identified modes (Modal), direct reconstruction (Direct), properness enforced reconstruction (Prop)

7.2 leads to the identification of the right and left eigenvectors:

$$\begin{aligned}\left[\phi_R^6\right] &= \begin{bmatrix} 0.0256 - 0.0322i & 0.0188 - 0.0201i \\ 0.0368 - 0.042i & -0.0381 + 0.0505i \end{bmatrix}, \\ \left[\phi_L^6\right] &= \begin{bmatrix} 0.0406 - 0.0511i & 0.0399 - 0.0425i \\ 0.0165 - 0.0164i & -0.0246 + 0.0278i \end{bmatrix}.\end{aligned} \tag{73}$$

The non symmetry of the system is clear. Once again, the properness enforcement induces small shifts in the identified complex modes:

$$\begin{aligned}\left[\tilde{\phi}_R^6\right] &= \begin{bmatrix} 0.0287 - 0.0287i & 0.0216 - 0.0173i \\ 0.0380 - 0.0411i & -0.0397 + 0.0491i \end{bmatrix}, \\ \left[\tilde{\phi}_L^6\right] &= \begin{bmatrix} 0.0427 - 0.0490i & 0.0413 - 0.0413i \\ 0.0190 - 0.0138i & -0.0269 + 0.0249i \end{bmatrix}.\end{aligned} \tag{74}$$

The changes in the complex shapes are illustrated in figure 10, and it can be observed that the changes mainly occur in the phase values, while the amplitudes of the vectors remain almost unchanged.

The direct inversion of the problem to estimate the values of the system matrices yields:

$$\begin{aligned}\left[M^6\right] = \begin{bmatrix} 0.543 & 0.0173 \\ 0.0350 & 0.628 \end{bmatrix}, \quad \left[C^6\right] = \begin{bmatrix} -18.4 & -1.25 \\ -1.05 & -20.6 \end{bmatrix}, \\ \left[K^6\right] = \begin{bmatrix} 2.59 \times 10^4 & 98.9 \\ -1.01 \times 10^3 & 3.07 \times 10^4 \end{bmatrix}.\end{aligned} \tag{75}$$

This is clearly not a reliable technique to obtain a physically meaningful damping matrix. Following properness enforcement, the reconstruction is much better:

$$\begin{aligned}\left[\tilde{M}^6\right] = \begin{bmatrix} 0.541 & 0.0168 \\ 0.0356 & 0.627 \end{bmatrix}, \quad \left[\tilde{C}^6\right] = \begin{bmatrix} 1.60 & -0.451 \\ 1.48 & 0.608 \end{bmatrix}, \\ \left[\tilde{K}^6\right] = \begin{bmatrix} 2.57 \times 10^4 & 87.8 \\ -988 & 3.06 \times 10^4 \end{bmatrix}.\end{aligned} \tag{76}$$

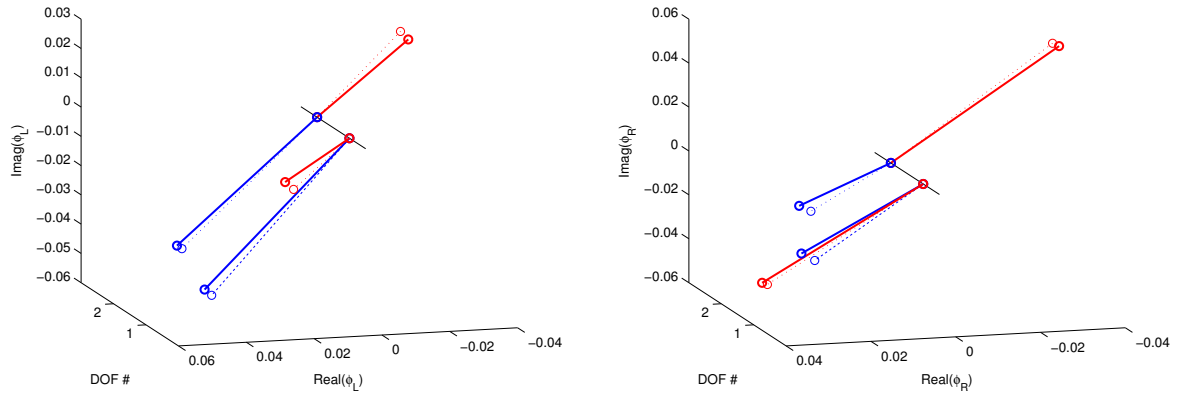

Figure 10: Right and left eigenmodes - original shapes (dashed lines), modified shapes (solid lines); mode 1 (blue), mode 2 (red)

The values of these matrices are now in accordance with the experimental conditions, namely: the mass matrix is almost unchanged, the damping matrix is slightly changed, according to the phase delays in the feedback loop, while the extradiagonal term of the stiffness matrix is very affected by the force feedback.

This analysis can be performed for several amplifier gain values in the feedback loop, in order to check the evolution of matrices terms when the gain changes. Figure 11 shows the results of the analysis. The mass matrix seems to be almost insensitive to the gain value, which is in accordance with the fact that the feedback is supposed to be proportional to the displacement. The extradiagonal terms are varying, but they are much smaller than the diagonal ones and this is physically reasonable. The stiffness matrix extradiagonal term K_{12} exhibits the largest evolution when the amplifiers gain changes and this is in accordance with the nature of the feedback, while the diagonal terms remain almost constant. Finally, even the behavior of the damping matrix is coherent now since there is a clear shift between the open loop configuration and the feedback loop configuration, which is due to the signal processing that induces phase delays which can be interpreted as damping effects. Nevertheless, once the feedback is considered, diagonal terms are almost constant, while an evolution of the extradiagonal terms can be observed due to the amplification of the feedback gain.

8. Conclusion

In this paper, the properness condition of complex modes is investigated and extended to non symmetric second order systems. An original methodology is proposed to optimally correct the experimental complex mode shapes in order to physically regularize the inverse procedure used to identify the system matrices. Three illustrations are presented. The first one is a purely numerical test based on an arbitrary simulated system. The second one is a numerical test resulting from the discretization of a rotordynamic application. The third one is an experimental test based on two coupled beams in bending with a non-collocated active feedback force. The trends observed on the three examples lead to the following conclusions:

- Enforcing the properness condition on the complex modes produces very slight changes in their components, and these changes mainly occur on the phase values while the amplitudes remain almost unchanged.
- When reconstructing a physical model from complex eigenvalues and eigenvectors, very small differences in the complex modes lead to very large differences in the system matrices, especially in the damping matrix. As a consequence, even a low level of noise affecting the complex modes can lead to a totally erroneous and non-physical estimation of the damping matrix.

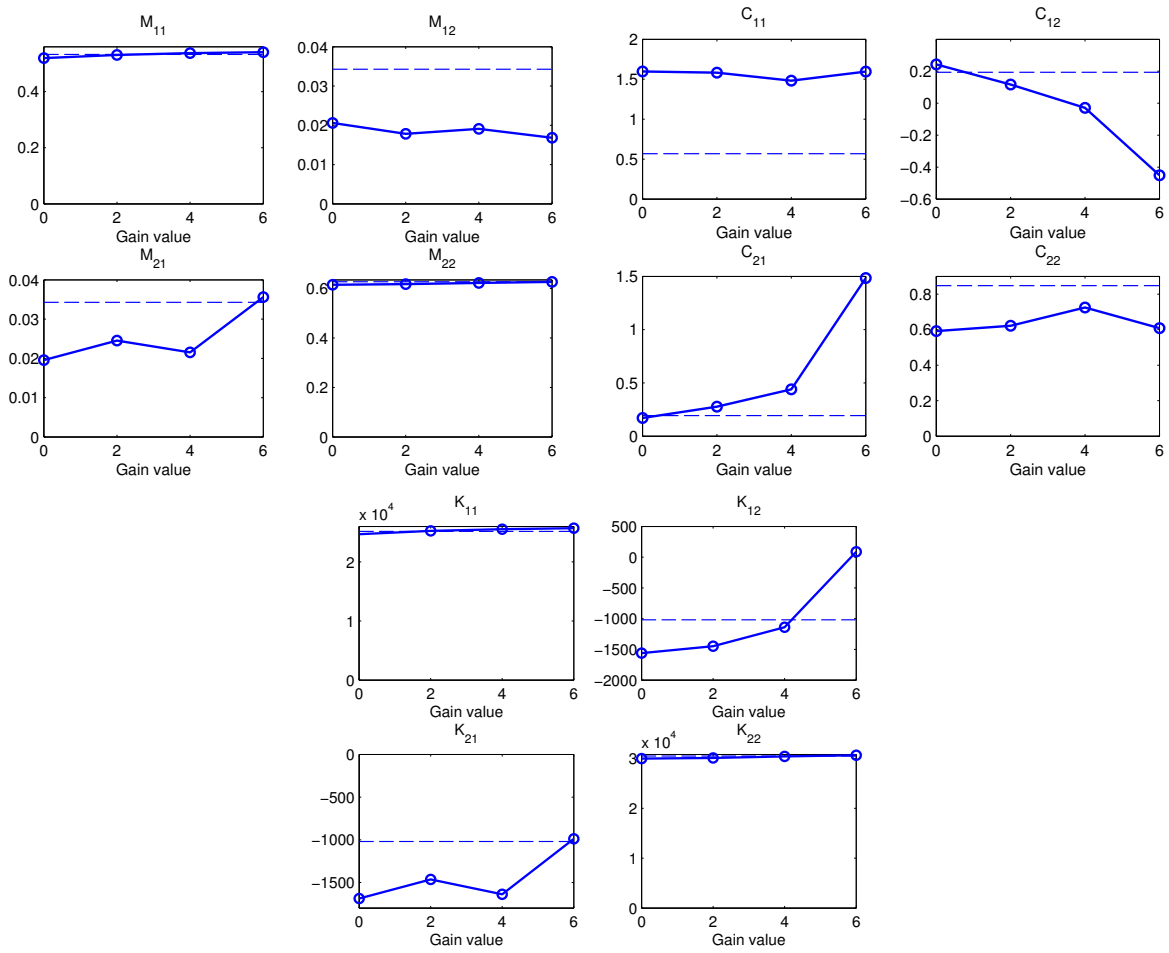

Figure 11: Evolution of mass, stiffness and damping matrices (SI units) terms versus gain value of amplifier (dashed line = open loop values)

- Modifying the complex modes by enforcing the properness condition is a good way to regularize the inverse problem. The reconstructed matrices and the derived FRFs show that the slight modifications applied to the eigenvectors drastically reduce the effect of uncertainties and allow the identification of physically meaningful matrices.

Finally, the enforcement of the properness condition on experimentally identified complex modes should be considered each time the reconstruction of a physical system is envisaged.

Appendix A. Numerical expressions of matrices

Appendix A.1. Direct reconstruction

$$[M_{dir}] = \begin{bmatrix} 9.20 \times 10^{-3} & -4.70 \times 10^{-1} & -2.01 \times 10^{-1} & -5.11 \times 10^{-2} & -1.62 \times 10^{-1} \\ 1.34 \times 10^{-2} & 9.50 \times 10^{-1} & 6.20 \times 10^{-1} & 1.19 \times 10^{-1} & 4.43 \times 10^{-1} \\ 1.06 \times 10^{-3} & 5.02 \times 10^{-1} & 1.23 \times 10^{-1} & 3.25 \times 10^{-2} & 1.40 \times 10^{-1} \\ 3.85 \times 10^{-3} & 3.49 \times 10^{-1} & 1.55 \times 10^{-1} & 3.57 \times 10^{-2} & 1.27 \times 10^{-1} \\ 9.49 \times 10^{-3} & 8.53 \times 10^{-1} & 4.50 \times 10^{-1} & 9.36 \times 10^{-2} & 3.39 \times 10^{-1} \end{bmatrix}, \tag{A.1}$$

$$[B_{dir}] = \begin{bmatrix} 3.83 \times 10^{0} & -2.66 \times 10^{1} & -2.81 \times 10^{1} & -7.34 \times 10^{0} & -1.75 \times 10^{1} \\ -9.87 \times 10^{0} & 9.71 \times 10^{0} & 3.11 \times 10^{1} & 1.08 \times 10^{1} & 1.82 \times 10^{1} \\ -3.97 \times 10^{0} & 4.33 \times 10^{1} & 3.94 \times 10^{1} & 9.75 \times 10^{0} & 2.54 \times 10^{1} \\ -3.04 \times 10^{0} & 1.88 \times 10^{1} & 2.07 \times 10^{1} & 5.53 \times 10^{0} & 1.30 \times 10^{1} \\ -7.98 \times 10^{0} & 3.01 \times 10^{1} & 4.06 \times 10^{1} & 1.18 \times 10^{1} & 2.49 \times 10^{1} \end{bmatrix}, \tag{A.2}$$

$$[K_{dir}] = \begin{bmatrix} 7.28 \times 10^{2} & -7.18 \times 10^{2} & -1.44 \times 10^{3} & -6.29 \times 10^{2} & -9.83 \times 10^{2} \\ -7.75 \times 10^{2} & 7.42 \times 10^{2} & 1.73 \times 10^{3} & 7.30 \times 10^{2} & 1.16 \times 10^{3} \\ -1.24 \times 10^{3} & 1.21 \times 10^{3} & 2.56 \times 10^{3} & 1.10 \times 10^{3} & 1.72 \times 10^{3} \\ -6.28 \times 10^{2} & 6.13 \times 10^{2} & 1.31 \times 10^{3} & 5.65 \times 10^{2} & 8.90 \times 10^{2} \\ -1.04 \times 10^{3} & 1.01 \times 10^{3} & 2.19 \times 10^{3} & 9.40 \times 10^{2} & 1.47 \times 10^{3} \end{bmatrix}. \tag{A.3}$$

Appendix A.2. Reconstruction with properness enforcement

$$[M_{prop}] = \begin{bmatrix} 1.26 \times 10^{-2} & -2.52 \times 10^{-1} & -9.79 \times 10^{-2} & -2.86 \times 10^{-2} & -7.91 \times 10^{-2} \\ 5.14 \times 10^{-3} & 7.98 \times 10^{-1} & 5.83 \times 10^{-1} & 1.09 \times 10^{-1} & 3.97 \times 10^{-1} \\ -2.23 \times 10^{-3} & 2.39 \times 10^{-1} & -1.79 \times 10^{-2} & 3.41 \times 10^{-3} & 3.42 \times 10^{-2} \\ 1.22 \times 10^{-3} & 2.14 \times 10^{-1} & 9.21 \times 10^{-2} & 2.20 \times 10^{-2} & 7.61 \times 10^{-2} \\ 2.72 \times 10^{-3} & 5.93 \times 10^{-1} & 3.39 \times 10^{-1} & 6.88 \times 10^{-2} & 2.44 \times 10^{-1} \end{bmatrix}, \tag{A.4}$$

$$[C_{prop}] = \begin{bmatrix} 2.05 \times 10^{0} & -1.30 \times 10^{1} & -1.60 \times 10^{1} & -3.89 \times 10^{0} & -9.42 \times 10^{0} \\ -8.53 \times 10^{0} & 1.97 \times 10^{1} & 3.56 \times 10^{1} & 1.09 \times 10^{1} & 2.17 \times 10^{1} \\ -1.87 \times 10^{0} & 2.57 \times 10^{1} & 2.51 \times 10^{1} & 5.57 \times 10^{0} & 1.54 \times 10^{1} \\ -1.95 \times 10^{0} & 1.24 \times 10^{1} & 1.49 \times 10^{1} & 3.69 \times 10^{0} & 9.01 \times 10^{0} \\ -5.82 \times 10^{0} & 2.31 \times 10^{1} & 3.26 \times 10^{1} & 8.93 \times 10^{0} & 1.97 \times 10^{1} \end{bmatrix}, \tag{A.5}$$

$$[K_{prop}] = \begin{bmatrix} 1.50 \times 10^{2} & -1.41 \times 10^{2} & -2.34 \times 10^{2} & -1.07 \times 10^{2} & -1.60 \times 10^{2} \\ -1.46 \times 10^{2} & 1.13 \times 10^{2} & 4.09 \times 10^{2} & 1.59 \times 10^{2} & 2.63 \times 10^{2} \\ -2.58 \times 10^{2} & 2.24 \times 10^{2} & 4.78 \times 10^{2} & 2.04 \times 10^{2} & 3.10 \times 10^{2} \\ -1.22 \times 10^{2} & 1.08 \times 10^{2} & 2.55 \times 10^{2} & 1.07 \times 10^{2} & 1.68 \times 10^{2} \\ -2.09 \times 10^{2} & 1.80 \times 10^{2} & 4.34 \times 10^{2} & 1.83 \times 10^{2} & 2.84 \times 10^{2} \end{bmatrix}. \tag{A.6}$$

References

[1] E. Balmès, New results on the identification of normal modes from experimental complex ones, Mechanical Systems and Signal Processing 11 (2) (1997) 229–243.

[2] K. Wyckaert, F. Augusztinovicz, P. Sas, Vibro-acoustical modal analysis: Reciprocity, model symmetry, and model validity, The Journal of the Acoustical Society of America 100 (1996) 3172–3181.

[3] Q. Zhang, G. Lallement, R. Fillod, Relations between the right and left eigenvectors of non-symmetric structural models. applications to rotors, Mechanical Systems and Signal Processing 2 (1) (1988) 97–103.

[4] F. Tisseur, K. Meerbergen, The quadratic eigenvalue problem, SIAM Review 43 (2) (2001) 235–286.

[5] N. Lieven, D. Ewins, Call for comments: a proposal for standard notation and terminology in modal analysis, The International Journal of Analytical and Experimental Modal Analysis 7 (2) (1992) 151–156.

[6] R. Fillod, J. Piranda, Research method of the eigenmodes and generalized elements of a linear mechanical structure, The Shock and Vibration Bulletin 48 (3) (1978) 5–12.

[7] H. Van der Auweraer, P. Guillaume, P. Verboven, S. Vanlanduit, Application of a fast-stabilizing frequency domain parameter estimation method, Journal of Dynamic Systems, Measurement, and Control 123 (2001) 651–658.
[8] A. Sestieri, S. Ibrahim, Analysis of errors and approximations in the use of modal co-ordinates, Journal of Sound and Vibration 177 (2) (1994) 145–157.
[9] Q. Zhang, G. Lallement, Comparison of normal eigenmodes calculation methods based on identified complex eigenmodes, Journal of Spacecraft and Rockets 24 (1) (1987) 69–73.
[10] A. Jameson, Solution of the equation $ax + xb = c$ by inversion of an $(m \times m)$ or $(n \times n)$ matrix, SIAM Journal on Applied Mathematics 16 (5) (1968) 1020–1023.
[11] L. Meirovitch, G. Ryland, A perturbation technique for gyroscopic systems with small internal and external damping, Journal of Sound and Vibration 100 (3) (1985) 393 – 408.
[12] I. Bucher, D. Ewins, Modal analysis and testing of rotating structures, Philosophical Transactions: Mathematical, Physical and Engineering Sciences 359 (1778) (2001) 61–96.